http://www.jstage.jst.go.jp/browse/biophysics

BIOPHYSICS

REVIEW

Vol. 7, pp. 113–122 (2011)
doi: 10.2142/biophysics.7.113

Importance of water entropy in rotation mechanism of F_1-ATPase

Takashi Yoshidome[1]

[1]*Institute of Advanced Energy, Kyoto University, Uji, Kyoto 611-0011, Japan*

Received August 1, 2011; accepted October 21, 2011

We briefly review our theoretical study on the rotation scheme of F_1-ATPase. In the scheme, the key factor is the water entropy which has been shown to drive a variety of self-assembly processes in biological systems. We decompose the crystal structure of F_1-ATPase into three sub-complexes each of which is composed of the γ subunit, one of the β subunits, and two α subunits adjacent to them. The β_E, β_{TP}, and β_{DP} subunits are involved in the sub-complexes I, II, and III, respectively. We calculate the hydration entropy of each sub-complex using a hybrid of the integral equation theory for molecular liquids and the morphometric approach. It is found that the absolute value of the hydration entropy follows the order, sub-complex I > sub-complex II > sub-complex III. Moreover, the differences are quite large, which manifests highly asymmetrical packing of F_1-ATPase. In our picture, this asymmetrical packing plays crucially important roles in the rotation of the γ subunit. We discuss how the rotation is induced by the water-entropy effect coupled with such chemical processes as ATP binding, ATP hydrolysis, and release of the products.

Key words: Asymmetric packing, water, hydration entropy, integral equation theory, morphometric approach

F_oF_1-ATP synthase is a molecular motor found in biological membranes. It is composed of a water-soluble part, F_1, and a membrane-embedded part, F_o. Coupled with proton transport across membranes, F_1-part of the synthase produces adenosine triphosphate (ATP) from adenosine diphosphate (ADP) and inorganic phosphate (Pi). F_1-ATPase, F_1-part of the synthase, is a rotary molecular motor induced by such chemical processes as the ATP binding, ATP hydrolysis, and release of products (ADP and Pi). In the present review, we focus on the $\alpha_3\beta_3\gamma$ complex in F_1-ATPase, which has widely been studied in single-molecule experiments[1–10]. According to the atomic-level crystal structures[11–14] of the $\alpha_3\beta_3\gamma$ complex, the $\alpha_3\beta_3$ subunits are arranged hexagonally around the γ subunit as shown in Figure 1. During the cycle of the chemical processes mentioned above, the γ subunit rotates in a counterclockwise direction when it is viewed from the F_o side[1]. The γ subunit performs a 120° step rotation during hydrolysis of a single ATP molecule[2]. This step is further resolved into 80° and 40° substeps. The 80° substep is induced by ATP binding[3] and/or release of ADP[5]. Subsequent ATP hydrolysis occurs in 1 ms without the rotation[4], which is followed by the 40° rotation accompanying release of Pi[6]. Release of ADP occurs during the 80° rotation[5]. The 80° and 40° dwells are referred to as catalytic and ATP-waiting dwells, respectively[4].

According to the crystal structure obtained by Abrahams *et al.*[11] in 1994 (Fig. 1), two of the β subunits named β_{TP} and β_{DP} are in closed conformation and the other one named β_E takes open conformation, respectively. AMP-PNP (an analog of ATP), and ADP are bound to the β_{TP} and β_{DP} subunits, respectively. Nothing is bound to the β_E subunit. The conformations of the three α subunits, on the other hand, are almost the same. (The three α subunits are named α_{TP}, α_{DP}, and α_E, respectively, as shown in the Fig. 1[11].) Most of the crystal structures which have been reported so far represent essentially the same characteristics though the substrates bound are different[12,13]. For example, in the crystal structure obtained by Bowler *et al.*[13] AMP-PNP binds to the β_{DP} sub-

Correspondence author: Takashi Yoshidome, Institute of Advanced Energy, Kyoto University, Uji, Kyoto 611-0011, Japan.
e-mail: t-yoshidome@iae.kyoto-u.ac.jp.

©2011 THE BIOPHYSICAL SOCIETY OF JAPAN

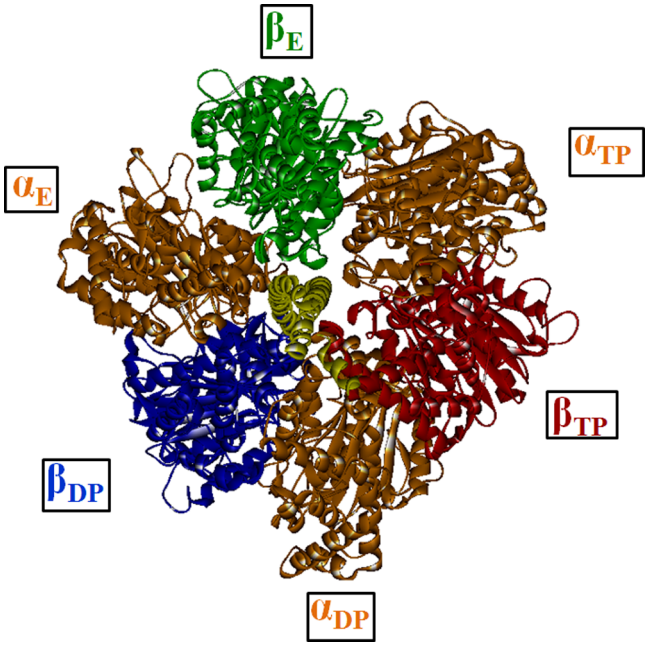

Figure 1 Ribbon representation of the $\alpha_3\beta_3\gamma$ complex viewed from the F_o side[11]. The γ subunit, represented by yellow ribbon, rotates in a counterclockwise direction[1]. This figure is drawn using the DS visualizer 2.5.

unit. (It has been experimentally shown that ATP is hydrolyzed in the β_{DP} subunit[7]. Thus, ATP binds to the β_{DP} subunit as well.) The 120° rotation of the γ subunit accompanies the interconversion of the β-subunit structures ($\beta_{DP}\rightarrow\beta_E$, $\beta_{TP}\rightarrow\beta_{DP}$, and $\beta_E\rightarrow\beta_{TP}$). The structures of the $\alpha_3\beta_3\gamma$ complex before and after the 120° rotation are the same. According to single-molecule experiments[7–9], most of the crystal structures are in the catalytic dwell state. This implies that the 40° rotation first occurs from the crystal structure, and the 80° rotation is then induced by the ATP binding and/or release of ADP.

Direct interactions between the γ and β subunits have been proposed as important factors for the rotation[14–16]. For example, Ma *et al.*[14] have suggested that the electrostatic interaction between Arg and Lys residues on the protruding portion of the γ subunit and negatively charged residues of the β subunit, known as the DELSEED motif, plays essential roles in the rotation. However, Hara *et al*. have shown that the rotation is not influenced by the mutation of a residue in the DELSEED motif to Ala[17], indicating that the electrostatic interaction between the γ and β subunits plays no important roles for the rotation. Furthermore, according to the experimental result by Fruike *et al.*[18], the γ subunit retains its rotation in the correct direction as well as its ATP-hydrolysis activity even when most of its axle including the DELSEED motif is removed. These experimental results imply that the rotation of the γ subunit is induced not by the direct interaction between the γ and β subunits but by another factor.

We have recently proposed the rotation scheme of the γ subunit based on the water-entropy effect[19]. In the present review, we briefly discuss how the water-entropy effect plays essential roles in the rotation of the γ subunit. We point out that the asymmetric packing found in the $\alpha_3\beta_3\gamma$ complex and the water-entropy effect provide important clues to the mechanism.

Water-entropy Effect in Biological Systems

Importance of water-entropy effect

Our recent theoretical analyses based on statistical thermodynamics of fluids have shown that the water entropy is the key quantity in elucidating the mechanism of such processes as protein folding/unfolding, molecular recognition between guest ligands and host enzymes, and aggregation of protein molecules like the amyloid-fibril formation[20,21]. As an illustration of the water-entropy effect, we consider a tight packing of the three side chains shown in Figure 2. The tight packing is induced by the excluded volume (EV) effect. Here the EV is defined as the volume which the centers of water molecules cannot enter[22]. In the left-hand side of Figure 2, for example, the EV corresponds to the molecular volume of the side chains plus the volume shown in gray. When a tight packing is formed, the EVs overlap, leading to a reduction of the EV. This decrease provides a corresponding increase in the total volume available to the translational displacement of the coexisting water molecules and in the number of accessible configurations of the water. Thus, tight packing leads to a gain in the water entropy. The native structure is the structure with almost the maximum water entropy[20,21]. Note that the interaction between protein atoms arising from the water-entropy effect is an indirect interaction via water molecules. According to the usual view[23], the water adjacent to a nonpolar group is entropically unstable, and protein folding is driven by the release of such unfavorable water to the bulk through the burial of nonpolar groups. However, we have shown that the entropic gain originating from this view is too small to reproduce the experimental result of apoplastocyanin (apoPC) folding[24]. Our recent studies on solvation thermodynamics have shown that "hydrophobic interaction" is driven primarily by the water entropy gain originating from the EV effect[20].

The above explanation is made under isochoric (constant-volume) condition while experiments are performed under isobaric (constant-pressure) one. However, it is experimentally known that the volume change upon folding ΔV is almost 0[25,26] (V is the partial molar volume of a protein, which is defined by the volume change upon insertion of a protein). Thus, protein folds under constant-volume and constant-pressure conditions. The above explanation is also valid under isobaric condition. The reason why ΔV is almost 0 is explained as follows. As discussed in ref 27 and in Supporting Information, V can be expressed as

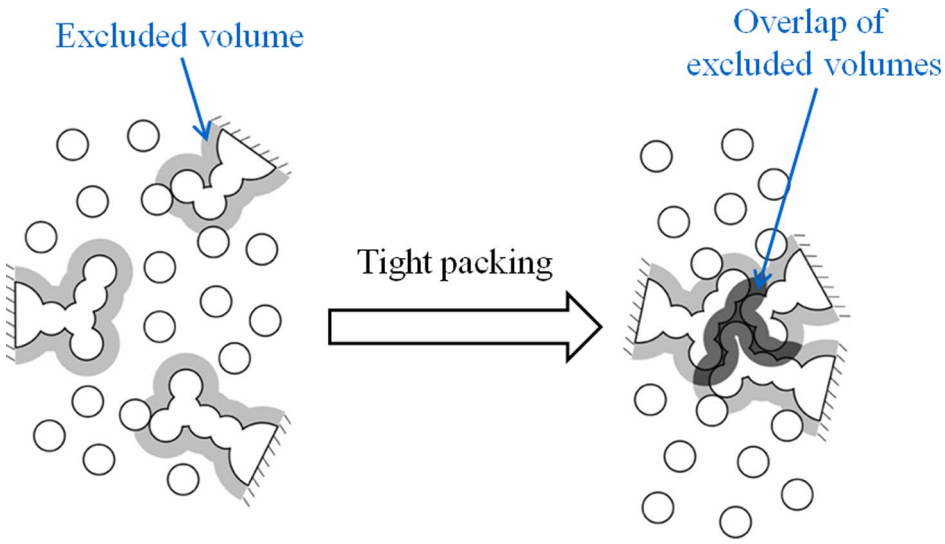

Figure 2 Close packing of three side chains. The excluded volume generated by a side chain is the volume occupied by the side chain itself plus the volume shown in gray. When side chains are closely packed, the excluded volumes overlap. The total volume available to the translational displacement of water molecules increases by the overlapped volume shown in black, leading to a water-entropy gain.

$$V \approx V_{ex} - \zeta A, \quad (1)$$

where V_{ex} is the EV, A is the water-accessible surface area, and ζ (>0) represents the average number density of water near the protein surface. When protein folds, both of V_{ex} and A reduce. The change of the volume upon folding becomes nearly 0 because the reduction of V_{ex} is almost cancelled out by the second term of Eq. (1). In the later subsection ("Hydration entropies of three sub-complexes"), we validate that the rotation mechanism of F_1-ATPase can also be discussed under isochoric condition.

The validity of our picture of protein folding has been shown in experiments. Here we discuss the experimental results by Terazima and coworkers. They developed a novel experimental technique which enables us to directly measure the enthalpic change, ΔH, upon protein folding at 298 K[26]. They showed that folding of apoPC accompanies an enthalpic loss of 870 kJ/mol that is very large. This indicates that the folding leads to a great gain of the water entropy which surpasses the enthalpic loss and a loss of the protein conformational entropy. The water-entropy gain upon folding can be estimated as follows[20,24]. The free-energy change upon folding, ΔG, can be expressed as $\Delta G = \Delta H - T(\Delta S_C + \Delta S)$ where ΔS_C is the conformational-entropy loss and ΔS is the water-entropy gain. The loss $-T\Delta S_C$ can be estimated to be in the range, 305 kJ/mol < $-T\Delta S_C$ < 956 kJ/mol[24]. It is assumed that the free-energy gain takes the most probable value shared by a number of proteins, −50 kJ/mol. Using $\Delta H = 870$ kJ/mol, the water-entropy gain is estimated to be in the range, −1876 kJ/mol < $-T\Delta S$ < −1225 kJ/mol. It follows that quite a large water-entropy gain occurs during the folding of apoPC. This large gain can never be explained by the contribution from the water molecules near the protein surface alone[20,21].

The enthalpic loss upon folding of apoPC can be explained as follows[20,21]. Protein folding leads to a lowering of the intramolecular energy by the formation of hydrogen bonds and salt bridges. We note, however, that the interaction between protein atoms and water molecules (e.g., protein-water hydrogen bonding) is lost upon the folding, leading to an increase in the protein-water interaction energy, the so-called dehydration penalty. The dehydration penalty is largely compensated if the intramolecular hydrogen bonds and/or salt bridges are formed. However, the formation is not always reached, giving rise to the dehydration penalty. The experimental result of apoPC indicates that the dehydration penalty is dominant and the enthalpy change is positive. We believe that the enthalpic loss upon folding occurs not only for apoPC but also for the other proteins. Although it has been reported for many proteins that the folding accompanies negative changes in the system enthalpy and entropy at room temperature[28], we have argued that it is an artifact arising from the experimental and estimation procedures for the changes employed. Details are described in ref 20.

Calculation of the hydration entropy based on the statistical thermodynamics of fluids

The quantity we focus on hereafter is the hydration entropy (HE), S, which represents the water-entropy loss upon the insertion of a solute with a prescribed structure. A larger absolute value of S, $|S|$, means a larger magnitude of the loss. The water-entropy change upon the conformational change of a solute from structure A to structure B is equal to the HE of structure B minus that of structure A.

The HE can be calculated by the angle-dependent inte-

gral equation theory[29–32], an elaborate theory of statistical-thermodynamics for molecular liquids. This theory allows us to calculate the thermodynamic quantities of hydration of a solute, as well as the density and orientational structures of water near the solute. In the theory, water is not a dielectric continuum but an ensemble of water molecules. The number of water molecules is infinitely large. The high reliability of the angle-dependent integral equation theory has been verified in a number of applications. For example, the hydration free energies of small nonpolar solutes calculated by the theory combined with the multipolar water model[29,30] are in perfect agreement with those from Monte Carlo simulations with the SPC/E and TIP4P water models[31]. The dielectric constant for bulk water, which is determined from the water-water orientational correlation functions, is in good agreement with the experimental data[31]. The theory is also capable of elucidating the hydrophilic hydration experimentally known[32].

Despite these successful results, the application of the angle-dependent integral equation theory to complex solute molecules like proteins is rather difficult due to the mathematical complexity. This problem can be overcome by combining it with the morphometric approach[33]. We calculate the HE by a hybrid of the angle-dependent integral equation theory combined with the multipolar water model[29,30] and the morphometric approach. Details of our hybrid method are described in refs 19, 24. In the calculation of HE, the (x, y, z)-coordinates of solute atoms are used as part of the input data to characterize each structure. The polyatomic structure, which is crucially important for the HE, is accounted for on the atomic level: All of the atoms constructing the protein complex and ATP (i.e., hydrogen, oxygen, carbon, nitrogen, sulfur, and phosphorus) are incorporated in the structures. It has been shown that by our hybrid method, very fast and accurate computation of the HE is possible. For example, we have calculated the water-entropy gain upon folding of apoPC[24]. In the calculation, we have assumed that the unfolded state comprises a set of random-coil structures. The HE of the unfolded state has been taken to be the average of the values for those structures. The water-entropy gain thus obtained is $-T\Delta S=-1658$ kJ/mol, which is certainly in the range estimated above, implying that the quantitative reproduction of the experimentally measured changes in thermodynamic quantities is successfully performed. Further, although in our hybrid method the polyatomic structure is accounted for on the atomic level, the calculation for $\alpha_3\beta_3\gamma$ complex with ~48000 atoms is finished only in a few minutes on the Xeon workstation. The calculation of the HE is performed under isochoric condition due to theoretical convenience. The validity of employing isochoric condition is described in the subsections "Importance of water-entropy effect" and "Hydration entropies of three sub-complexes.

Rotation Scheme of the γ Subunit based on the Water-entropy Effect

Asymmetric packing in the $\alpha_3\beta_3\gamma$ complex

It has been pointed out that the packing of the $\alpha_3\beta_3\gamma$ complex in crystal structures is highly asymmetrical. For example, using an all-atom molecular dynamics (MD) simulation, Ito and Ikeguchi[34] have analyzed packing at the interfaces between adjacent subunits in terms of the number of stable contacts. The stable contacts are defined as the inter-subunit residue pairs maintaining their inter-atomic distances less than 4.5 Å for 98% of snapshots in the MD trajectory. The number of stable contacts can be a measure of tightness of packing at the interfaces between adjacent subunits. Ito and Ikeguchi have found that the packing at the interfaces between β_{DP}, adjacent α subunits, and γ subunit is especially tight, implying that the four subunits are strongly interacted (See Fig. 3(a)). Experimental studies have shown that in the structure illustrated in Figures 1 and 3(a), the rotation of the γ subunit occurs upon a structural change of β_{DP}, the catalytically active subunit[7,9]. It is likely that perturbation of the tight packing by the structural change of β_{DP} induces the movement of the γ subunit.

We have considered that the asymmetric packing is driven primarily by the water-entropy effect and that it should be analyzed in terms of the water entropy. In our study, we use the same crystal structure of the $\alpha_3\beta_3\gamma$ complex as that employed by Ito and Ikeguchi (the $\alpha_3\beta_3\gamma$ complex of the crystal structure from Bovine Heart Mitochondria (PDBID: 2JDI)[13]). In the crystal structure, all subunits except for the β_E subunit have AMP-PMP and Mg^{2+}. Neither of the nucleotide nor Mg^{2+} is bound to the β_E subunit. We replace AMP-PMP by ATP because the results by single-molecule experiments have indicated that most of the crystal structures are in the catalytic dwell state[7,9].

Measures of tight packing between adjacent subunits

As a first step, we investigate whether the results of the MD simulation by Ito and Ikeguchi can be reproduced in terms of the water-entropy effect. As a measure of tight packing between adjacent subunits, we calculate $\Delta S_{ij} \equiv S_{ij} - S_i - S_j$ where S_{ij} is the HE of subunit pair *i-j* and S_i is the HE of subunit *i*. (*i-j*=α_{TP}-β_E, α_E-β_E, α_E-β_{DP}, α_{DP}-β_{TP}, α_{TP}-β_{TP}, α_{DP}-β_{DP}, α_{DP}-γ, α_{TP}-γ, α_E-γ, β_E-γ, β_{TP}-γ, and β_{DP}-γ.) The calculation procedure is as follows: (i) we first take an arbitrary subunit pair *i-j* from the crystal structure; (ii) the HE of subunit pair *i-j* is calculated; (iii) we calculate the HE of each subunit (subunit *i* or *j*); and (iv) ΔS_{ij} is calculated. ΔS_{ij} represents the water-entropy gain upon formation of subunit pair *i-j*. It becomes larger as the tightness of interface packing between subunit pair *i-j* increases because the tight packing between adjacent subunits leads to the large reduction of the EV. Thus, ΔS_{ij} is a measure of the tightness like the number of stable contacts calculated in the MD simulation[34].

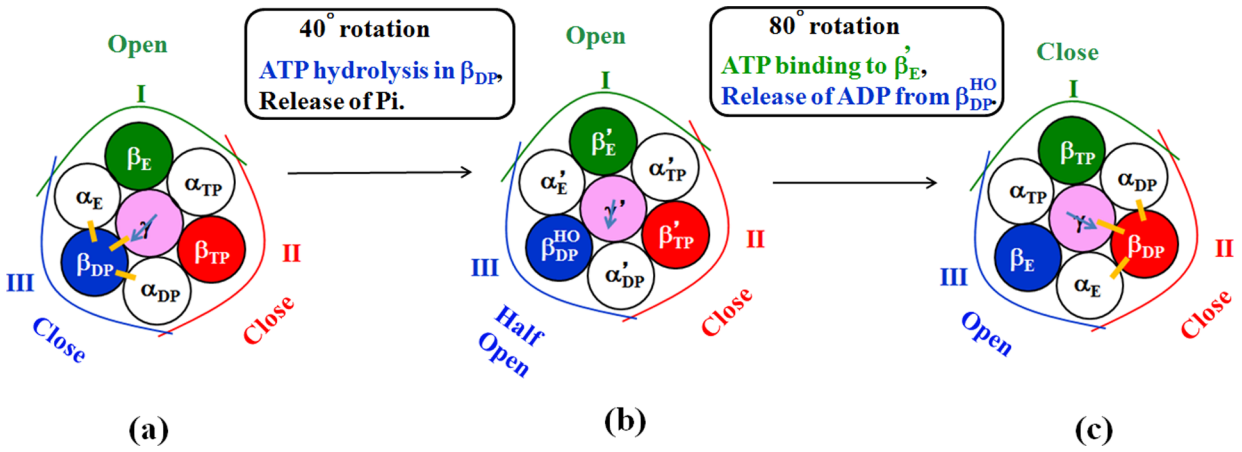

Figure 3 Summary of experimental results using schematic representation of the $\alpha_3\beta_3\gamma$ complex viewed from the F_o side. (a) Schematic representations of the crystal structure shown in Figure 1. The yellow lines represent that the packing in two adjacent subunits is especially tight[34]. Three circular arcs denote sub-complexes I (green), II (red), and III (blue), respectively. The definition of each sub-complex is described in "Hydration entropies of three sub-complexes". The other figures represent (b) the overall conformation after the first 40° rotation of the γ subunit and (c) the overall conformation after the second 80° rotation of the γ subunit. Primes are added to the subunits in (b) because their conformations should be different from those in (a). The definition of the arrow at the center of the γ subunit is shown in the original paper[19].

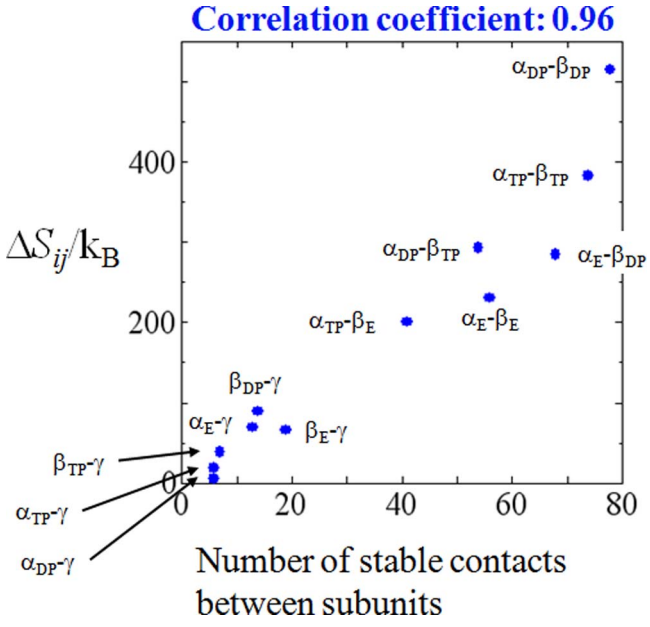

Figure 4 Comparison between the numbers of stable contacts estimated by the MD simulation with all-atom potentials[34] and the water-entropy gain upon the formation of subunit pair *i*-*j*, S_{ij}/k_B. Each value is shown in the original paper[19] and in the supporting information of the paper of Ito and Ikeguchi[34].

As shown in Figure 4, $\Delta S_{ij}/k_B$ is highly correlated with the number of stable contacts obtained in the MD simulation by Ito and Ikeguchi[34] (the correlation coefficient is 0.96). Thus, the framework of the results of the MD simulation is successfully reproduced using our hybrid method focused on the water-entropy effect. In the MD simulation, quite a long computation is inevitable. On the other hand, the calculation of the HE for one subunit pair is finished only in a few seconds by our hybrid method. Nevertheless, the packing characteristics estimated by the MD simulation can beautifully be reproduced, which is remarkable.

Hydration entropies of three sub-complexes

The 120° rotation of the γ subunit is induced by overall conformational changes of the β subunits as well as changes in the interface packing between subunits. For this reason, we define the following three sub-complexes as shown Figure 3(a):

Sub-complex I: γ, β_E, α_E, and α_{TP},
Sub-complex II: γ, β_{TP}, α_{TP}, and α_{DP},
Sub-complex III: γ, β_{DP}, α_{DP}, and α_E.

We name the sub-complexes in terms of their positions in the crystal structure. For example, when the γ subunit rotates by 120° (see Fig. 3(c)), the arrangement changes and sub-complex III now comprises γ, β_E, α_E, and α_{TP}. We first generate the three sub-complexes from the crystal structure (see Fig. 5) and then calculate the HE of each sub-complex. To make the number of the atoms in each sub-complex impartial, we add the HE of ATP-Mg^{2+} to the HE of sub-complex I. The values of the HE of the three sub-complexes are shown in Table 1. It follows that the value of $|S|/k_B$ (k_B is the Boltzmann constant) is in the order, sub-complex III < sub-complex II < sub-complex I. Therefore, the water-entropy loss upon the insertion of sub-complex III is the smallest.

Since the conformations of the complex before and after the 120° rotation of the γ subunit are the same, there is no water-entropy change upon the 120° rotation. However, the free energy of the system reduces by the free-energy decrease by ATP hydrolysis. It is interesting to note that as

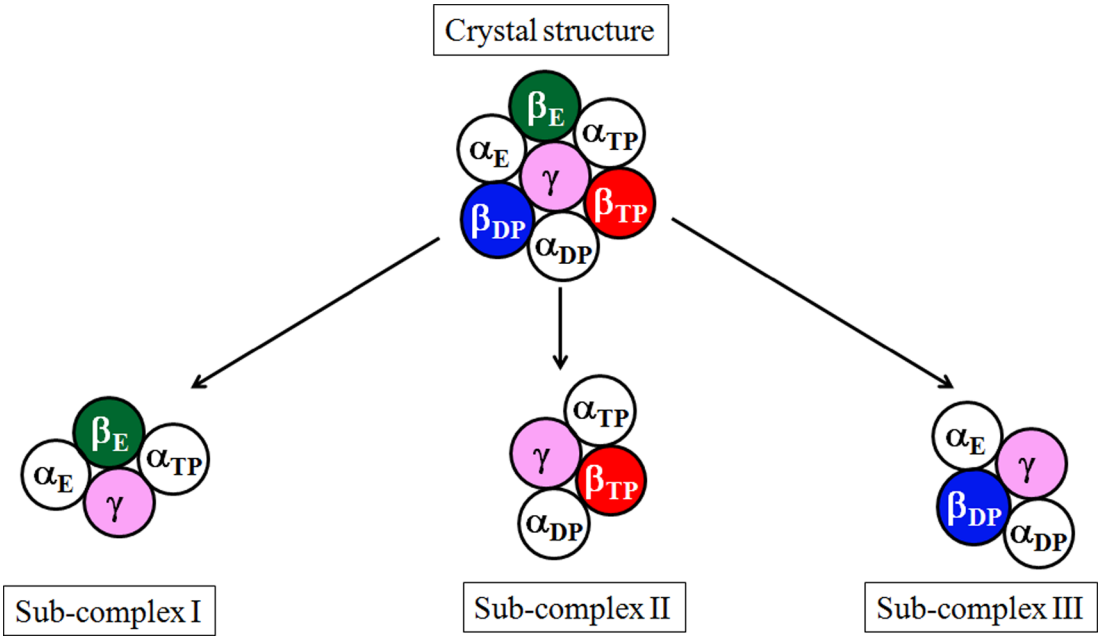

Figure 5 Schematic representation of the generation of the three sub-complexes from the crystal structure.

Table 1 Hydration entropy, S/k_B, for each sub-complex.

	I	II	III
S/k_B	−61245	−61028	−60619

The definition of each sub-complex is described in "Hydration entropies of three sub-complexes".

observed in Table 1 the rotation leads to the water-entropy gains of $217k_B$ and $409k_B$ (540 kJ/mol and 1010 kJ/mol at 298 K, respectively) in sub-complex I and sub-complex II, respectively, and to the water-entropy loss of $626k_B$ (1550 kJ/mol at 298 K) in sub-complex III. This result indicates that the rotation leads to tighter packing in sub-complexes I and II, and looser packing in sub-complex III, respectively. It should be noted that the gains and loss are quite large. Any loss caused in one of the sub-complexes during the rotation is compensated by the gains occurring in the other sub-complexes. Without this compensation, the system would undergo a significantly large free-energy barrier hindering a smooth rotation of the γ subunit.

As described in "Calculation of the hydration entropy based on the statistical thermodynamics of fluids", the calculation of the HE is performed under isochoric condition. This can be validated by a discussion which is similar that given in "Importance of water-entropy effect". As packing becomes tighter in sub-complexes I and II upon rotation, both of V_{ex} and A reduce. Since the reduction of V_{ex} is almost cancelled out by the second term of Eq. (1), change in V of sub-complexes I and II upon rotation is quite small. This is also true for sub-complex III: a looser packing upon rotation leads to an increase in V_{ex} and A. Due to the cancelation of an increase in V_{ex} by the second term of Eq. (1), V of sub-complex III is also almost unchanged upon rotation. The rotation mechanism can reasonably be discussed under isochoric condition.

Rotation scheme predicted from the analysis on the water-entropy effect

We first summarize the experimental results that have been reported.

(1) Figure 3(a) is the crystal structure. Both of β_{TP} and β_{DP} are in closed conformations with ATP binding while β_E adopts an open conformation[11–13].

(2) From Figure 3(a), the γ subunit rotates by 40° (Fig. 3(a) → Fig. 3(b))[6]. During the rotation, the hydrolysis of ATP in β_{DP}[4] and release of Pi[6] occur, with the result that β_{DP} changes its conformation into a half-open one[9]. The β subunit with the changed conformation is denoted by β_{DP}^{HO}. The $\alpha_3\beta_3\gamma$ complex now takes the overall conformation shown in Figure 3(b). Primes are added to the subunits in Figure 3(b) because their conformations should be different from those in Figure 3(a). Although the crystal structure corresponding to Figure 3(b) has not been determined yet, it has been shown by single-molecule experiments[9] that β_E', β_{DP}^{HO}, and β_{TP}' are in open, half-open, and closed conformations, respectively. Here we comment on the time of Pi release. There are two probable pictures[6]: Pi produced from ATP hydrolysis is immediately released[35], or the Pi release is suspended for the next 120° rotation[10]. The release occurs from the β_{DP} subunit in the former picture while it occurs from the β_E subunit in the latter one. Although the time of the Pi release is still an open question, our rotation mecha-

nism discussed below is not influenced by this uncertainty.

(3) From Figure 3(b), the γ subunit rotates by 80° (Fig. 3(b) → Fig. 3(c)). During the rotation, the conformational changes[9], β_E'→β_{TP} and $\beta_{DP}{}^{HO}$→β_E, occur due to the ATP binding[3] and release of ADP[6], respectively. The $\alpha_3\beta_3\gamma$ complex now takes the overall conformation shown in Figure 3(c), which is the same as that of the crystal structure (see Fig. 3(a)). However, the free energy of the system G_{System} in Figure 3(c) is lower than that in Figure 3(a) by the free-energy decrease arising from ATP hydrolysis.

The experimental results summarized above can be explained in terms of the water entropy as follows. (We consider the situation where the ATP concentration is much higher than the ADP and Pi concentrations.)

(1) Figure 3(a): Two of the β subunits are in closed conformation and the other one takes an open conformation. In this situation, the $\alpha_3\beta_3\gamma$ complex is packed with high asymmetry so that the water entropy in the presence of the $\alpha_3\beta_3\gamma$ complex can be made as high as possible. The tightest packing is formed in sub-complex III. The reasons why such an asymmetric packing is formed are due to an asymmetric nature of the γ subunit and to nonuniform binding of nucleotides to the three β subunits. Here we discuss why such asymmetric packing is formed by the water-entropy effect. As explained in Figure 2, it is desired for a protein or a complex of proteins that the backbones and side chains be tightly packed as a three-dimensional jigsaw puzzle. However, this is not always possible. When the overall, impartial tight packing is not achievable in a protein, the portions which can tightly be packed are chosen for the preferential tight packing. This action is taken by the water-entropy effect. For example, the native structure of yeast frataxin[36] has a large valley and a tail as shown in Figure 6. Nevertheless, $|S|$ of the native structure is almost minimized[37] because the other portions are tightly packed. If an impartial packing was undertaken, the valley and/or the tail could be removed but the resultant packing would become rather loose, causing a larger value of $|S|$.

(2) Figure 3(a) → Figure 3(b): The conformational change of β_{DP} into $\beta_{DP}{}^{HO}$ gives rise to a looser packing in sub-complex III. This conformational change would cause a decrease in the water entropy of sub-complex III. For suppressing the decrease in the water entropy, the 40° rotation of the γ subunit in a counterclockwise direction is required (the angle 40° comes from the experimental observation). As a consequence, the packing in sub-complex II becomes tighter, leading to a water-entropy gain. The water-entropy loss in sub-complex III is thus almost compensated by this water-entropy gain, leading to a smooth rotation of the γ subunit. Further, since Pi is highly charged, its release leads to a large decrease in the hydration energy. Thus, G_{System} in Figure 3(b) becomes lower than that in Figure 3(a).

(3) Figure 3(b) → Figure 3(c): The conformational changes of β_E' and $\beta_{DP}{}^{HO}$ (β_E'→β_{TP} and $\beta_{DP}{}^{HO}$→β_E) are induced by the ATP binding and ADP release, respectively.

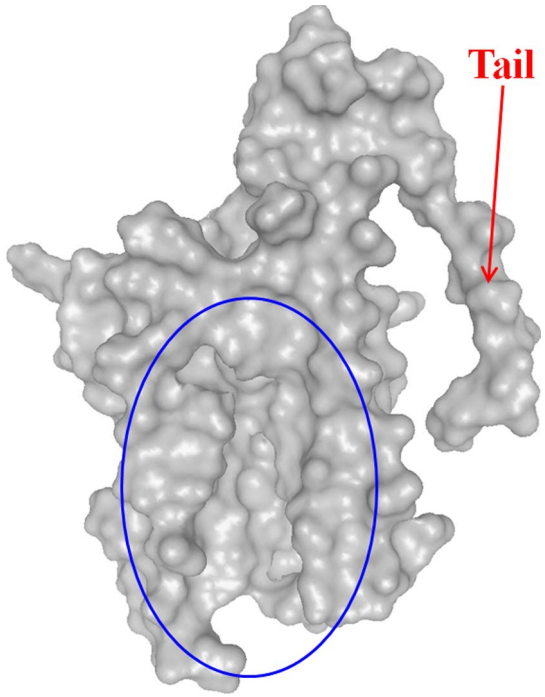

Figure 6 Solvent-surface representation of the native structure of yeast frataxin (PDBID: 2ga5)[36] drawn by the DS visualizer 2.5. This structure has the large valley marked by the blue ellipse and the tail pointed by the red arrow.

The latter one would lead to a water-entropy loss in sub-complex III. On the other hand, a water-entropy gain occurs in sub-complex I by the former conformational change. Further, the packing in sub-complex II would become tighter by the 80° rotation of the γ subunit, leading to a water-entropy gain. The γ subunit would rotate smoothly by the compensation between the water-entropy loss in sub-complex III and these water-entropy gains. By the 80° rotation, the overall conformation of the $\alpha_3\beta_3\gamma$ complex becomes that as shown in Figure 3(c). Since two of the β subunits are now in closed conformations and the other takes an open conformation, the conformation stabilized as shown in Figure 3(a) is recovered. Sub-complex II in Figure 3(c) forms the tightest packing which is the same as that in sub-complex III in Figure 3(a). The absolute value of the HE of each sub-complex in Figure 3(c) is in the order, sub-complex II < sub-complex I < sub-complex III. The water entropy of the $\alpha_3\beta_3\gamma$ complex remains the same upon the overall-conformational change, Figure 3(a) → Figure 3(c), but G_{System} is lowered by the free-energy decrease due to ATP hydrolysis. We remark that G_{System} is in the order, Figure 3(a) > Figure 3(b) > Figure 3(c).

Concluding Remarks and Perspective

We have reviewed our rotation scheme of the γ subunit[19]. In our scheme, the asymmetric packing of the $\alpha_3\beta_3\gamma$ complex and the water-entropy effect arising from the transla-

tional displacement of water molecules induce the rotation during the chemical processes of the ATP binding, ATP hydrolysis, and release of products. Here we give perspectives to construct the complete rotation mechanism in the following two paragraphs.

In the present review, we have constructed the rotation scheme by analyzing the HEs of the three sub-complexes in the crystal structure corresponding to that shown in Figure 3(a). In order to validate the rotation scheme we have proposed and to construct the complete rotation mechanism, the conformations which appear between the conformations before and after the 120° rotation, especially the conformation corresponding to that shown in Figure 3(b), are required. However, the crystal structure corresponding to Figure 3(b) has not been determined yet. Instead, the conformation after 16° rotation from Figure 3(a) is found in the crystal structures of yeast F_1-ATPase[13]. As part of the demonstration of the validity of our rotation mechanism, we are now analyzing the water-entropy change in yeast F_1-ATPase during 16° rotation of the γ subunit. The compensation in terms of the water entropy, which is explained in the text, actually occurs during 16° rotation (details will be presented in a future article). As a future work, the conformations of the $\alpha_3\beta_3\gamma$ complex which appear between the conformations before and after the 120° rotation could be generated using an MD simulation.

We have focused on the water-entropy effect in the present review. The strong correlation between the results obtained by our theoretical method and by an MD simulation (Fig. 4) validates the predominance of the water-entropy effect. In order to construct the complete rotation mechanism, however, the effect of the energetic component on the rotation scheme should be clarified. At present, we have the following picture of the energetic component. Decreases in the intramolecular energy by tight packing occur in sub-complexes I and II upon rotation of the γ subunit. However, such decreases are somewhat compensated by increases in the protein-water interaction energy. This is also true for sub-complex III: an increase in the intramolecular energy by a looser packing is compensated by a decrease in the protein-water interaction energy. Thus, the differences among the sub-complexes in the energetic component should be substantially smaller than those in the water entropy: The differences in the free energy are still considerably large due to the large difference in the water entropy. In order to validate the picture, we are now analyzing the energetic terms for subunit pairs and sub-complexes by the MD simulation coupled with the method of energy representation[38]. Details will be presented in a future article.

Recently, using high-speed atomic force microscopy (AFM), Uchihashi *et al*. have shown that even in the $\alpha_3\beta_3$ complex (*i.e*., *without* the γ subunit) the three β subunits undergo the same cyclic conformational changes in the same rotary direction as in the case of the $\alpha_3\beta_3\gamma$ complex[39]. In accordance with this result, we calculate the HEs of three sub-complexes without the γ subunit[19] (in this case, sub-complex III, for example, comprises β_{DP}, α_{DP}, and α_E). We have found that the order of the HE is the same as that in the case with the γ subunit shown in Table 1. Our result and the experimental one by Uchihashi *et al*. suggest that the asymmetric nature of the $\alpha_3\beta_3$ complex is crucially important for the rotation.

The water-entropy effect has been shown to be the key factor in elucidating the mechanisms of folding and unfolding (pressure[27,40], cold[37,41], and heat[42,43] denaturations) of proteins. We have recently reported that the unidirectional movement of a linear-motor protein along a filament[44] and the insertion of a big solute into and from a vessel constructed by biopolymers[45,46] are also driven by the water-entropy effect. Thus, the water-entropy effect is imperative for a variety of biological processes sustaining life.

Acknowledgments

The author thanks Prof. M. Kinoshita, Prof. M. Ikeguchi, and Dr. Y. Ito for the collaboration in the present study. The computer program for the morphometric approach was developed by Profs. R. Roth, Y. Harano, and M. Kinoshita. This work was supported mainly by Grants-in-Aid for Scientific Research on Innovative Areas (Nos. 20118004 and 20118519).

References

1. Noji, H., Yasuda, R., Yoshida, M. & Kinosita Jr., K. Direct observation of the rotation of F_1-ATPase. *Nature* **386**, 299–302 (1997).
2. Yasuda, R., Noji, H., Kinosita Jr., K. & Yoshida, M. F_1-ATPase is a highly efficient molecular motor that rotates with discrete 120° steps. *Cell* **93**, 1117–1124 (1998).
3. Yasuda, R., Noji, H., Yoshida, M., Kinosita Jr., K. & Itoh, H. Resolution of distinct rotational substeps by submillisecond kinetic analysis of F_1-ATPase. *Nature* **410**, 898–904 (2001).
4. Shimabukuro, K., Yasuda, R., Muneyuki, E., Hara, K. Y., Kinosita Jr. K. & Yoshida, M. Catalysis and rotation of F_1 motor: Cleavage of ATP at the catalytic site occurs in 1 ms before 40° substep rotation. *Proc. Natl. Acad. Sci. USA* **100**, 14731–14736 (2003).
5. Nishizaka, T., Oiwa, K., Noji, H., Kimura, S., Muneyuki, E., Yoshida, M. & Kinosita Jr., K. Chemomechanical coupling in F_1-ATPase revealed by simultaneous observation of nucleotide kinetics and rotation. *Nat. Struct. Mol. Biol*. **11**, 142–148 (2004).
6. Adachi, K., Oiwa, K., Nishizaka, T., Furuike, S., Noji, H., Itoh, H., Yoshida, M. & Kinosita Jr., K. Coupling of Rotation and Catalysis in F_1-ATPase Revealed by Single-Molecule Imaging and Manipulation. *Cell* **130**, 309–321 (2007).
7. Okuno, D., Fujisawa, R., Iino, R., Hirono-Hara, Y., Imamura, H. & Noji, H. Correlation between the conformational states of F_1-ATPase as determined from its crystal structure and single-molecule rotation. *Proc. Natl. Acad. Soc. USA* **105**, 20722–20727 (2008).
8. Sieladd, H., Rennekamp, H., Engelbrecht, S. & Junge, W. Functional Halt Positions of Rotary F_OF_1-ATPase Correlated with Crystal Structures. *Biophys. J*. **95**, 4979–4987 (2008).

9. Masaike, T., Koyama-Horibe, F., Oiwa, K., Yoshida, M. & Nishizaka, T. Cooperative three-step motions in catalytic subunits of F_1-ATPase correlate with 80° and 40° substep rotations. *Nat. Struct. Mol. Biol*. **15**, 1326–1333 (2008).
10. Watanabe, R., Iino, R. & Noji, H. Phosphate release in F_1-ATPase catalytic cycle follows ADP release. *Nat. Chem. Biol*. **6**, 814–820 (2010).
11. Abrahams, J. P., Leslie, A. G., Lutter, R. & Walker, J. E. Structure at 2.8 Å resolution of F_1-ATPase from bovine heart mitochondria. *Nature* **370**, 621–628 (1994).
12. Kabaleeswaran, V., Puri, N., Walker, J. E., Leslie, A. G. W. & Mueller, D. M. Novel features of the rotary catalytic mechanism revealed in the structure of yeast F_1-ATPase. *EMBO. J*. **25**, 5433–5442 (2006).
13. Bowler, M. W., Montgomery, M. G., Leslie, A. G. W. & Walker, J. E. Ground state structure of F_1-ATPase from bovine heart mitochondria at 1.9 Å resolution. *J. Biol. Chem*. **282**, 14238–14242 (2007).
14. Ma, J., Flynn, T. C., Cui, Q., Leslie, A. G. W., Walker, J. E. & Karplus, M. A dynamic analysis of the rotation mechanism for conformational change in F_1-ATPase. *Structure* **10**, 921–931 (2002).
15. Koga, N. & Takada, S. Folding-based molecular simulations reveal mechanisms of the rotary motor F_1-ATPase. *Proc. Natl. Acad. Sci. USA* **103**, 5367–5372 (2006).
16. Pu, J. & Karplus, M. How subunit coupling produces the -subunit rotary motion in F_1-ATPase. *Proc. Natl. Acad. Sci. USA* **105**, 1192–1197 (2008).
17. Hara, K. Y., Noji, H., Bald, D., Yasuda, R., Kinosita Jr., K. & Yoshida, M. The role of the DELSEED motif of the subunit in rotation of F_1-ATPase. *J. Biol. Chem*. **275**, 14260–14263 (2000).
18. Furuike, S., Hossain, M.D., Maki, Y., Adachi, K., Suzuki, T., Kohori, A., Itoh, H., Yoshida, M. & Kinosita Jr., K. Axle-less F_1-ATPase rotates in the correct direction. *Science* **319**, 955–958 (2008).
19. Yoshidome, T. Ito, Y., Ikeguchi, M. & Kinoshita, M. Rotation mechanism of F_1-ATPase: Crucial importance of water-entropy effect. *J. Am. Chem. Soc*. **133**, 4030–4039 (2011).
20. Kinoshita, M. Importance of translational entropy of water in biological self-assembly processes like protein folding. *Int. J. Mol. Sci*. **10**, 1064–1080 (2009).
21. Kinoshita, M. Roles of translational motion of water molecules in sustaining life. *Front. Biosci*. **14**, 3419–3454 (2009).
22. Lee, B. & F. M. Richards, F. M. The Interpretation of Protein Structures: Estimation of Static Accessibility. *J. Mol. Biol*. **55**, 379–400 (1971).
23. Kauzmann, W. Some factors in the interpretation of protein denaturation. *Adv. Protein Chem*. **14**, 1–63 (1959).
24. Yoshidome, T., Kinoshita, M., Hirota, S., Baden, N. & Terazima, M. Thermodynamics of apoplastocyanin folding: Comparison between experimental and theoretical results. *J. Chem. Phys*. **128**, 225104(1–9) (2008).
25. Chalikian, T. V. & Breslauer, K. J. On volume changes accompanying conformational transitions of biopolymers. *Biopolymers* **39**, 619–626 (1996).
26. Baden, N., Hirota, S., Takabe, T., Funasaki, N. & Terazima, M. Thermodynamical properties of reaction intermediates during apoplastocyanin folding in time-domain. *J. Chem. Phys*. **127**, 175103(1–12) (2007).
27. Harano, Y. & M. Kinoshita, M. Crucial importance of translational entropy of water in pressure denaturation of proteins. *J. Chem. Phys*. **125**, 024910(1–10) (2006).
28. Liu, L., Yang, C. & Guo, Q.-X. A study on the enthalpy-entropy compensation in protein unfolding. *Biophys. Chem*. **84**, 239–251 (2000).
29. Kusalik P. G. & Patey, G. N. On the molecular theory of aqueous electrolyte solutions. I. The solution of the RHNC approximation for models at finite concentration. *J. Chem. Phys*. **88**, 7715–7738 (1988).
30. Kusalik, P. G. & Patey, G. N. The solution of the reference hypernetted-chain approximation for water-like models. *Mol. Phys*. **65**, 1105–1119 (1988).
31. Kinoshita, M. Molecular origin of the hydrophobic effect: Analysis using the angle-dependent integral equation theory. *J. Chem. Phys*. **128**, 024507(1–14) (2008)..
32. Kinoshita, M. & Yoshidome, T. Molecular origin of the negative heat capacity of hydrophilic hydration *J. Chem. Phys*. **130**, 144705(1–11) (2009).
33. Roth, R., Harano, Y. & Kinoshita, M. Morphometric approach to the solvation free energy of complex molecules. *Phys. Rev. Lett*. **97**, 078101(1–4) (2006).
34. Ito, Y. & Ikeguchi, M. Structural fluctuation and concerted motions in F_1-ATPase: A molecular dynamics study. *J. Comp. Chem*. **31**, 2175–2185 (2010).
35. Shimo-Kon, R., Muneyuki, E., Sakai, H., Adachi, K., Yoshida, M. & Kinosita Jr., K. Chemo-mechanical coupling in F_1-ATPase revealed by catalytic site occupancy during catalysis. *Biophys. J*. **98**, 1227–1236 (2010).
36. Adinolfi, S., Nair, M., Politou, A., Bayer, E., Martin, S., Temussi, P. & Pastore, A. The factors governing the thermal stability of frataxin orthologues: How to increase a protein's stability. *Biochemistry* **43**, 6511–6518 (2004).
37. Oshima, H., Yoshidome, T., Amano, K. & Kinoshita, M. A theoretical analysis on characteristics of protein structures induced by cold denaturation. *J. Chem. Phys*. **131**, 205102(1–11) (2009).
38. Matubayasi, N. Free-energy analysis of solvation with the method of energy representation. *Front. Biosci*. **14**, 3536–3549 (2009).
39. Uchihashi, T., Iino, R., Ando, T. & Noji, H. High-speed atomic force microscopy reveals rotary catalysis of rotorless F_1-ATPase. *Science* **333**, 755–758 (2011).
40. Yoshidome, T., Harano, Y. & Kinoshita, M. Pressure effects on structures formed by the entropically driven self-assembly: Illustration for denaturation of proteins. *Phys. Rev. E* **79**, 011912(1–10) (2009).
41. Yoshidome, T. & Kinoshita, M. Hydrophobicity at low temperatures and cold denaturation of a protein. *Phys. Rev. E* **79**, 030905(1–4) (2009).
42. Amano, K., Yoshidome, T., Harano, Y., Oda, K., & Kinoshita, M. Theoretical analysis on thermal stability of a protein focused on the water entropy. *Chem. Phys. Lett*. **474**, 190–194 (2009).
43. Oda, K., Kodama, R., Yoshidome, T., Yamanaka, M., Sambongi, Y. & Kinoshita, M. Effects of heme on the thermal stability of mesophilic and thermophilic cytochromes *c*: Comparison between experimental and theoretical results. *J. Chem. Phys*. **134**, 025101 (2011).
44. Amano, K., Yoshidome, T., Iwaki, M., Suzuki, M., Kinoshita, M. Entropic potential field formed for a linear-motor protein near a filament: Statistical-mechanical analyses using simple models. *J. Chem. Phys*. **133**, 045103(1–11) (2010).
45. Amano, K. & Kinoshita, M. Entropic insertion of a big sphere into a cylindrical vessel. *Chem. Phys. Lett*. **488**, 1–6 (2010).
46. Amano, K. & Kinoshita, M. Model of insertion and release of a large solute into and from a biopolymer complex. *Chem. Phys. Lett*. **504**, 221–224 (2011).

Supporting Information

Theoretical framework of the partial molar volume

The partial molar volume V can be obtained by the Kirkwood-Buff formula[1]

$$V = \iiint \{1 - g_{US}(x, y, z)\}\, dxdydz\,, \qquad (1)$$

where $g_{US}(x, y, z)$ represents the microstructure of the solvent near the protein surface and is referred to as the reduced density profile. It has the physical meaning that the number of solvent molecules within the volume element $dxdydz$ is given by $\rho_S g_{US}(x, y, z)dxdydz$. At distances which are sufficiently far from the protein surface, $g_{US} \to 1$. No overlap of an atom in the protein and a water molecule is allowed, and at positions where such an overlap occurs $g_{US}=0$. The values of V obtained by Eq. (1) are in accord with the experimentally measured values[2]. For example, V of lysozyme calculated is 11,600 cm^3/mol that is in good agreement with the average of the experimentally measured value, 10,100 cm^3/mol.

It is convenient to divide the term in the right hand of Eq. (1) into the integrations inside and outside the core regions[2]. Inside the core region, due to the overlap of the protein and solvent, the protein-solvent potential is infinitely large and $g_{US}=0$. It follows that the integration inside the core region equals the excluded volume, V_{ex}, which the centers of solvent molecules cannot enter. The integration outside the core region takes a negative value because a layer within which the solvent density is higher than in the bulk is formed near both of hydrophobic[3] and hydrophilic surfaces[4]. Since the higher density is almost limited to the first layer (*i.e.*, the thickness of the denser layer reaches only about half of the solvent diameter), the integration over region 2 can be approximated by $-\zeta A$ where ζ (>0) is a parameter representing the average number density of water within the layer and A is the water-accessible surface area (ASA). Thus, we can express Eq. (1) as

$$V \approx V_{ex} - \zeta A \qquad (2)$$

Equation (2) indicates that V is smaller than V_{ex} due to the second term in the right-hand side of Eq. (2).

References

1. Kirkwood, J. G. & Buff, F. P. The statistical mechanical theory of solutions. I. *J. Chem. Phys*. **19**, 774–777 (1951).
2. Harano, Y. & Kinoshita, M. Crucial importance of translational entropy of water in pressure denaturation of proteins. *J. Chem. Phys*. **125**, 024910(1–10) (2006).
3. Kinoshita, M. Water structure and phase transition near a surface. *J. Sol. Chem*. **33**, 661–687 (2004).
4. Kinoshita, M. & Yoshidome, T. Molecular origin of the negative hydrophilic hydration. *J. Chem. Phys*. **130**, 144705(1–11) (2009).